ARPES: novel effect in the energy and momentum distributions

J. R. Schrieffer, Arno P. Kampf

ARPES: NOVEL EFFECT IN THE ENERGY AND MOMENTUM DISTRIBUTIONS

J.R. SCHRIEFFER

National High Magnetic Field Laboratory and Department of Physics Florida State University, Tallahassee, Florida 32306, U.S.A.

A.P. KAMPF

Institut für Theoretische Physik, Universität zu Köln 50937 Köln, Germany

Abstract—The physical origin of two effects, i.e. shadow bands and three peaked energy spectra in the ARPES and inverse photoemission spectra of strongly correlated electron systems, such as the cuprates, are discussed. Shadow bands arise from quasi elastic exchange Bragg scattering from residual antiferromagnetic spin correlations in the paramagnetic phase. Three peaked energy spectra arise as a superposition of the central Landau quasi particle peak of the weakly correlated system and the upper and lower band peaks split by the SDW and/or Mott Hubbard pseudo gap 2Δ of the strongly correlated system. The coexistence of these three resonances is explained in terms of quasi particles propating in a medium with $\Sigma(k, \omega)$ exhibiting strong anomalous dispersion, i.e. multiple fermionic modes for fixed k.

The spectral function $A(\mathbf{k}, \omega)$ governing photo– and inverse photoemission in antiferromagnets, like superconductors, is qualitatively different from that in weakly correlated metals in that two peaks at quasi particle energies $\pm E_\mathbf{k} = \pm\sqrt{\epsilon_\mathbf{k}^2 + \Delta_\mathbf{k}^2}$ occur in the energy distribution for fixed $\mathbf{k}$ in the former while a single Landau quasi particle peak occurs at $\epsilon_\mathbf{k}$ in the latter. Furthermore, because of Bragg exchange scattering, the antiferromagnet (AF) exhibits quasi particle states

$$\gamma_{\mathbf{k}s}^c = u_\mathbf{k} c_{\mathbf{k}s} + 2sv_\mathbf{k} c_{\mathbf{k}+\mathbf{Q}s} \quad \text{(particle-like)}$$

$$\gamma_{\mathbf{k}s}^v = v_\mathbf{k} c_{\mathbf{k}s} - 2su_\mathbf{k} c_{\mathbf{k}+\mathbf{Q}}s \quad \text{(hole-like)} \quad (1)$$

which are linear combinations of the Landau–like states, where $\mathbf{k}$ is inthe first magnetic Brillouin zone, $\mathbf{Q}$ is the AF wavevector and $s = \pm\frac{1}{2}$ the spin quantum number along the AF sublattice direction. Thus, for fixed binding energy $E_\mathbf{k}$, one has electron emission with momenta $\mathbf{k}$ and $\mathbf{k} + \mathbf{Q}$ ("magnetic umklapp") with relative intensities $v_\mathbf{k}^2$ and $u_\mathbf{k}^2$. In contrast, in fermi liquids electron emission occurs only at $\mathbf{k}$ (except for crystal lattice umklapp at $\mathbf{k} + \mathbf{G}$, where $\mathbf{G}$ is a reciprocal crystal lattice vector).

AF spin fluctuation systems, with spin correlation length L_s and characteristic frequency ω_0, were shown by the present authors to exhibit novel spectral features $A(\mathbf{k}, \omega)$ in both the momentum and energy distributions,[1] namely:

(1) **for fixed energy** ω, broadening magnetic umklapp beams occur in photoemission andare centered around $\mathbf{k} + \mathbf{Q}$, with integrated intensity, $u_\mathbf{k}^2$,where $\mathbf{Q}$ is magnetic reciprocal lattice vector of the ordered AF, and

(2) **for fixed k**, *three* peaks occur in the energy distribution corresponding to the coexistence of the split peaks $\pm E_\mathbf{k}$ of the ordered AF phase *plus* the Landau peak of the fermi liquid phase.

The magnetic umklapp effect, i.e. presence of spectral

weight for $\mathbf{k}$ *not only* in the first magnetic Brillouin zone (MBZ) is termed the shadow band effect. With an impressive experimental setup this shadow band effect (i) has recently been reported in room temperature ARPES experiments on the cuprate superconductor $Bi\,2212$.[2,3] While shadow band effects are clear from the physical point of view, less clear is how a Landau quasi particle peak (admittedly of small spectral strength) survives well into the spin fluctuation (SF) regime, where the SF frequency ω_0 is small compared to 2Δ and band tails into the pseudo gap are small. The explanation of this phenomenon is given below in terms of anomalous dispersion. This situation is analogous for the acoustic modes of an organ pipe containing a driven sound mode.

Beginning with the ordered AF, the mean field energy bands are plotted in Fig. 1a in the *reduced* zone scheme, Fig. 1b in the *extended* zone scheme, and in Fig. 1c the *periodic* zone scheme. It is the latter representation which smoothly connects with the SF regime. To illustrate this point, we plot the AF bands as a function of Bloch momentum $\mathbf{k}$ (labelling the $c_{\mathbf{k}s}$ of the non–magnetic crystal schematically as opposed to the magnet eigenstate "Neel momentum") labelling γ_k in the ordered AF. The shading of the lines represents the spectral weight at each $\mathbf{k}$ and ω, namely

$$u_\mathbf{k}^2 = \frac{1}{2}\left(1 + \frac{\epsilon_\mathbf{k}}{E_\mathbf{k}}\right) \quad \text{(upper band)}$$

$$v_\mathbf{k}^2 = \frac{1}{2}\left(1 - \frac{\epsilon_\mathbf{k}}{E_\mathbf{k}}\right) \quad \text{(lower band)} \quad (2)$$

with $u_\mathbf{k}^2$ and $v_\mathbf{k}^2$ plotted in Fig. 1d.

Working with a periodic Kondo or spin fermion model

$$H = \sum_{\mathbf{k}s} \epsilon_\mathbf{k} n_{\mathbf{k}s} + J\sum_i \psi_i^\dagger \underline{\sigma} \psi_i \cdot \mathbf{S}_i + H_{ss} \quad (3)$$
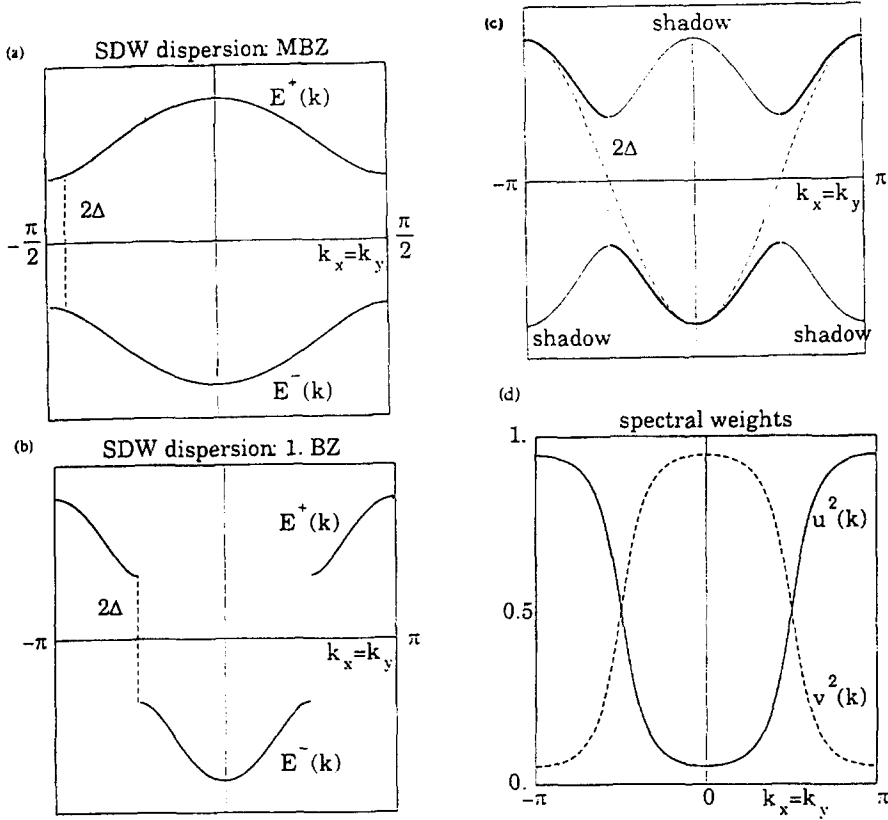
Fig. 1. Energy bands in the SDW state along the zone diagonal $k_x = k_y$ in (a) the reduced magnetic Brillouin zone, (b) the extended first Brillouin zone, and (c) the repeated zone scheme. In (c) the shading of the lines represents their relative spectral weight. The dashed line indicates the expected dispersion in the spin fluctuation phase without long range magnetic order. (d) Spectral weight functions $u^2()$ and $v^2(\mathbf{k})$ along the zone diagonal.

or alternatively with a one–band Hubbard model, and assuming a simple model form of the spin propagator

$$\chi(\mathbf{q}, \omega) = -\lambda^2 a^2(\Gamma) \sum_{\mathbf{Q}=(\pm\pi,\pm\pi)} \frac{\Gamma}{(q_x - Q_x)^2 + \Gamma^2} \times$$
$$\times \frac{\Gamma}{(q_y - Q_y)^2 + \Gamma^2} \int g(v) \frac{2v}{\omega^2 - v^2 + i\delta} dv \quad (4)$$

the authors found the electron self–energy

$$\Sigma(\mathbf{k}, \omega) = -iU^2 \frac{1}{N} \sum_{\mathbf{q}} \int \frac{dv}{2\pi} \chi(\mathbf{q}, v) G_0(\mathbf{k} - \mathbf{q}, \omega - v) \quad (5)$$

shows anomalous behavior compared to that of a conventional fermi liquid;[1] examples are shown in Fig. 2. In Eq. (4) Γ is the inverse of the spin–spin correlation length and the frequency distribution function $g(\omega)$ is chosen linear up to a characteristic SF cutoff frequency ω_0. The prefactor $a(\Gamma)$ normalizes the area of the Lorentzians around the AF wavevectors to unity. The authors showed why these results are very insensitive to the form of $\chi(q, \omega)$, so long as χ is strongly peaked about $\mathbf{q} \simeq \mathbf{Q}$ and ω_0 is small compared to the fermionic pseudo gap 2Δ, as for the MMP[4] forms of χ.

In the AF phase, the mean field self–energy is

$$\Sigma^{AF}(\mathbf{k}, \omega) = \frac{\Delta^2}{\omega + \epsilon_{\mathbf{k}}} \quad (6)$$

as shown in Fig. 3a. $\epsilon_{\mathbf{k}}$ is the tight binding dispersion for the noninteracting electrons, e.g. $\epsilon_{\mathbf{k}} = -2t (\cos k_x + \cos k_y)$ for the square lattice. The divergence of Σ at $\epsilon_{\mathbf{k}}$ pushes up energy states above $\epsilon_{\mathbf{k}}$ and pushes down states below $\epsilon_{\mathbf{k}}$. This is the cause of the gap 2Δ, as in a superconductor. In contrast, in a fermi liquid, Σ typically depends weakly on $\mathbf{k}$ and Σ has a negative slope near the chemical potential $\mu \equiv 0$ as shown in Fig. 3b, pushing down high energy states and up low energy states near $\omega = 0$; i.e. a mass enhancement $m^*/m 1$. The remarkable result that both features are simultaneously present in this antiferromagnetical metal spin fluctuation phase, as shown in Fig. 3c, although the negative slope near $\omega = 0$ extends only to the characteristic spin fluctuation energies $\simeq \pm\omega_0$ significant strength (spectral weight) exists only for $\mathbf{k}$ near $\mathbf{k}_F$, i.e. $|k - k_F| < \omega_0/v_F$, where $v_F = |\nabla\epsilon_{\mathbf{k}}|_{k_F}$.

Since the poles of $G(\mathbf{k}, \omega)$ give the quasi particle energies,

$$G^{-1}(\mathbf{k}, \omega) = \omega - \epsilon_{\mathbf{k}} - \Sigma(\mathbf{k}, \omega) = 0 \quad (7)$$

it appears from Fig. 3c that five peaks would appear in $A(\mathbf{k}, \omega)$ for fixed $\mathbf{k}$. It is readily seen that poles labelled 2 and
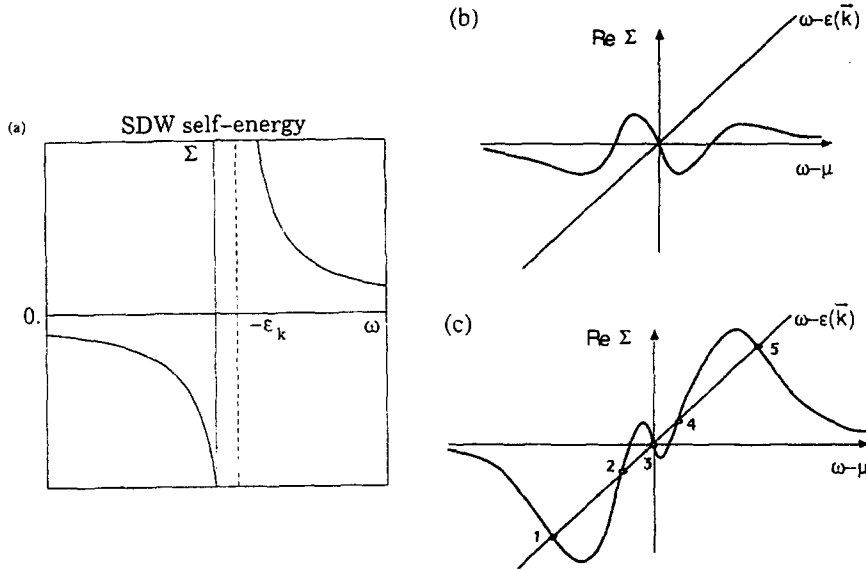
Fig. 3. (a) Real part of the mean-field self-energy in the SDW state.(b) Typical shape for the frequency dependence of $\Re\Sigma$ in a Landau fermi liquid. (c) Modified shape of $\Re\Sigma$ in the spin fluctuation regime. Indicated in the figure are the intersections of $\Re\Sigma$ with $\omega - \epsilon_k$ for $k = k_F$ determining the peak energies of the spectral function.
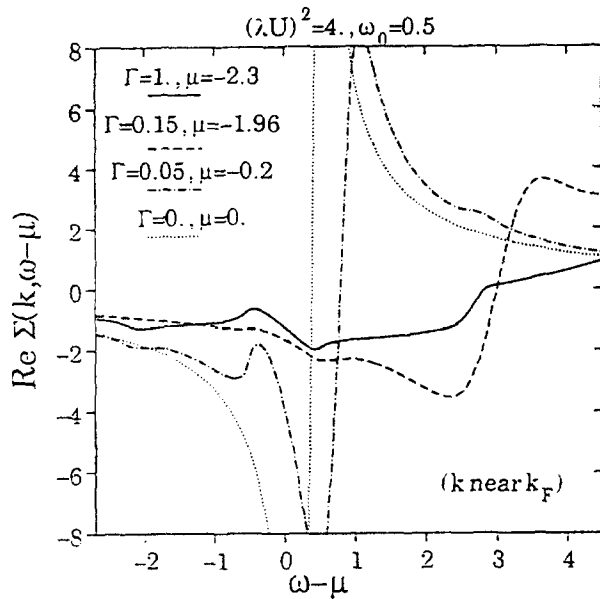

Fig. 2. The real part of the one-loop self-energy calculated with the model susceptibility Eq. (4) for the parameter sets as indicated in the figure. Energies are measured in units of the hopping amplitude t for the tight binding dispersion on a square lattice. $\Sigma(k, \omega)$ has been calculated on a 108×108 lattice for a momentum k along the diagonal of the Brillouin zone (i.e. $k_x = k_y$); k has been chosen as the momentum closest below k_F along the zone diagonal.

4 are heavily damped and contribute only to the incoherent background, while poles 1 and 5 are the AF lower and upper bands and pole 3 is the Landau peak, whose weight z_3 is extremely small for $L_s \gg a \equiv 1$ (the crystal lattice spacing).

Therefore, in addition to the shadow contours in $A(\mathbf{k}, \omega)$ for fixed ω there is also a novel structure in the binding energy distribution at fixed momentum $\mathbf{k}$. In essence, the single peak Landau–like spectrum for very short L_s crosses over to the two–peak spectrum of the ordered SDW in a smooth manner. Namely, rather than the Landau peak at ϵ_k splitting into two peaks at the energies $E_k^\pm = \pm\sqrt{\epsilon_k^2 + \Delta^2}$ of the energies of the SDW phase we found that the $E_k^\pm$ peaks grow out of the incoherent background of the Landau spectrum, while the Landau peak continues to exist but with strongly reduced weight.[1]

The corresponding evolution of the spectral function $A(\mathbf{k}, \omega - \mu)$ as calculated from the model susceptibility Eq. (4) for a specific parameter set is demonstrated in Fig. 4. The density of states (DOS) which follows from the momentum integration of the spectral functions is shown in Fig. 5. Remarkably, once the chemical potential has moved into the energy range near the top of the valence band for intermediate and small $\Gamma = 1/L_s$ a peak in the DOS appears close to μ, quite similar to what is found in the numerical studies of the 2D Hubbard model.[5,6]

Of course, in a complete analysis of a microscopic SF model the dynamical spin susceptibility $\chi(\mathbf{q}, \omega)$ would have to be determined self consistently from the model. L_s would diverge for the AF parent compound for $\mu = 0$ and μ would be negative for finite L_s and $\omega_0 > 0$ in the hole doped material. Both L_s and μ would have a model specific dependence on the doping. Nevertheless, it has proven to be instructive to vary L_s, ω_0 and μ independently as a test for the sensitivity of $A(\mathbf{k}, \omega)$ to each of these parameters.

In numerical simulations for the 2D Hubbard model the chemical potential has been found to move very rapidly with hole doping from $\mu = 0$ in the AF insulator at half–filling into the energy range of the former SDW valence band.[5] We therefore have analyzed the electronic spectrum which
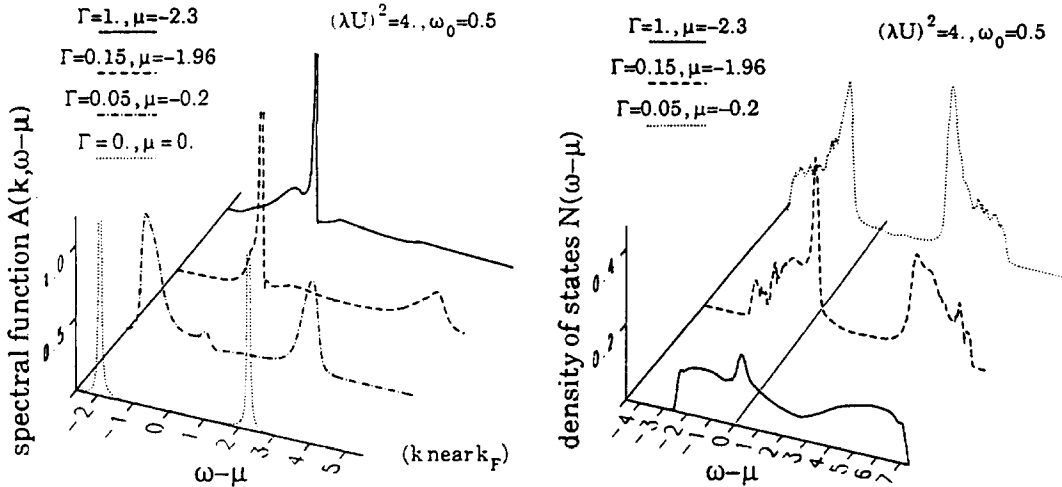
Fig. 4. Frequency dependence of the spectral functions $A(k, \omega - \mu)$ for the same parameter set as in Fig. 2. The figure shows the evolution with decreasing spin-spin correlation length $L_s = 1/\Gamma$ from the two-peak structure of the SDW state (dotted line) and to the three-peak structure at $L_S = 20$ (dashed dotted line), and to the Landau like single peak spectrum at $L_S = 1$ (solid line). In the intermediate case (dashed line) the chemical potential is located in the energy range of the remnant structure of the valence SDW band.
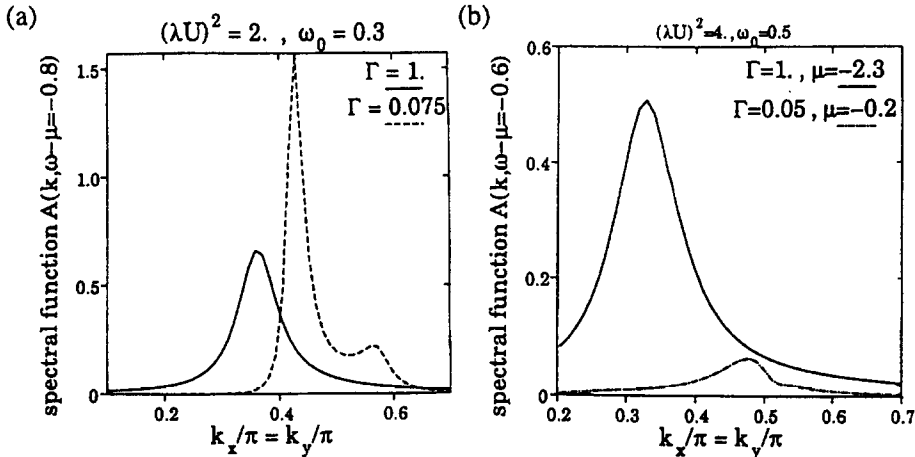

Fig. 5. Densities of states for the same parameter sets as in Figs. 1,2, and 3 showing the evolution with increasing spin-spin correlation length to the pseudogap structure at large L_S. For the three different parameter sets the electron densities are 0.59 (solid line), 0.71 (dashed dotted line), and 0.98 (dotted line), respectively.

follows from the self–energy Eq. (5) for the situation of a rapidly moving μ at low hole doping under the assumption that fairly long range AF correlations [i.e. a small Γ in the model susceptibility Eq. (4)] still persist. This motivates the specific choice of parameters used in the calculations for Figs. 2,4, and 5.

Clearly, the correlation of Γ with μ determines the doping window in which the three–peak spectrum is realized. Specifically, for the 2D Hubbard model the doping window around half–filling for the three–peak structure must be tiny. For the small lattice sizes explored so far in numerical simulation studies the three–peak spectrum may be not observable, since on the small lattices already a single hole represents a doping concentration of a few percent and the three–peak spectrum may be inaccessible. Our phenomeno-

logical model analysis is therefore not in conflict with the numerical simulation studies for the 2D Hubbard model.

The situation is different for the observability of the shadow band effect (i) when ARPES spectra are scanned in momentum. Figure 6 shows the k dependence along the Brillouin zone diagonal at a fixed frequency (binding energy) below the chemical potential for the same parameter set as used above. Only a single Landau like quasiparticle peak is visible when the magnetic correlation length is comparable to the lattice spacing, i.e. for $\Gamma = 1$. The additional shadow peak rises with increasing L_s at a large momentum above k_F due to the magnetic umklapp effect described above mixing momentum states $|k\rangle$ and $|k + Q\rangle$. Note, however, that in the case of the three–peak spectrum the central small weight quasiparticle peak does not have a shadow structure in the
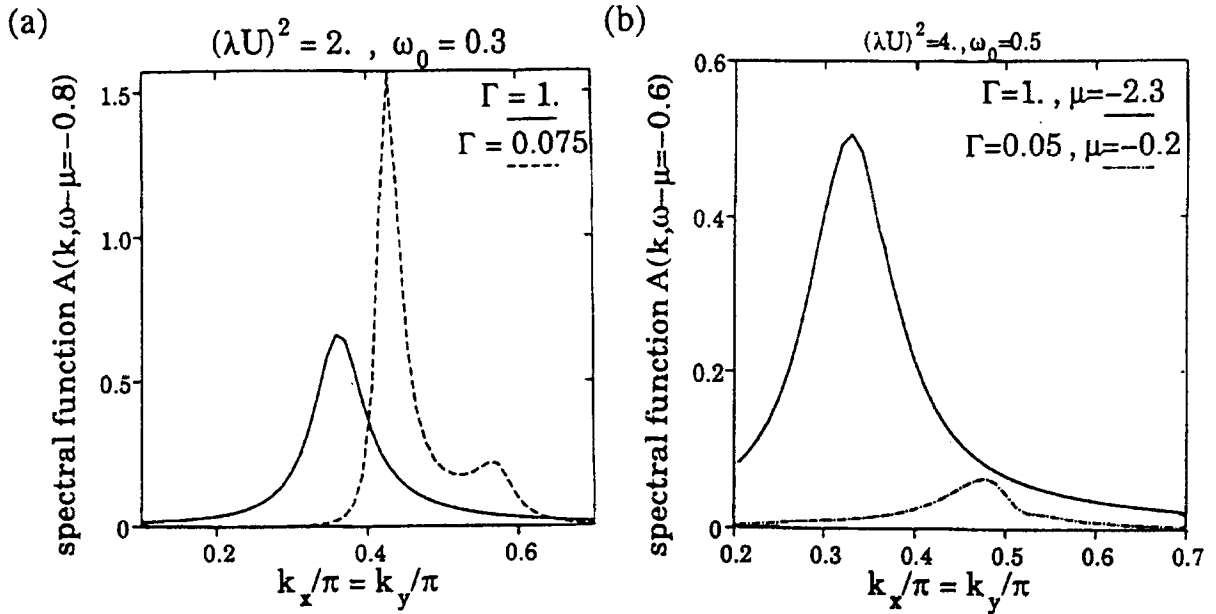
(a)

$(\lambda U)^2 = 2.$, $\omega_0 = 0.3$

$\Gamma = 1.$
$\Gamma = 0.075$

spectral function $A(k, \omega - \mu = -0.8)$

$k_x/\pi = k_y/\pi$

(b)

$(\lambda U)^2 = 4.$, $\omega_0 = 0.5$

$\Gamma = 1.$, $\mu = -2.3$
$\Gamma = 0.05$, $\mu = -0.2$

spectral function $A(k, \omega - \mu = -0.6)$

$k_x/\pi = k_y/\pi$

Fig. 6. Spectral functions $A(k, \omega - \mu)$ for a fixed frequency below the chemical potential plotted as a function of momentum k along the diagonal of the Brillouin zone. For the Landau like spectrum [solid line in Figs. (a) and (b)] only a single peak appears in the ARPES spectrum. However, for sufficiently long range spin correlations [dashed line in (a)] a shadow peak with smaller weight appears at larger momentum above k_F besides the dominant quasiparticle peak. Note that no shadow structure of the Landau peak appears in the three-peak spectrum (dash–dotted line in Fig. (b), compared also with Fig. 4 for the same parameter set).

momentum dependence of the spectral function.

Thus, one sees that the persistence of Landau peak well into the spin fluctuation phase, $L_s \gg 1$, and its coexistence with the Mott-Hubbard-Slater upper and lowerbands is simply understood in terms of quasi particles propagating in a highly dispersive medium, in that $\Sigma(k, \omega)$ has a pole at $\omega \cong \epsilon_k$. This property leads to multiple zeros of $G^{-1}(k, \omega)$ with nonzero residues of G (fermion quasi particlemodes) just as several (boson) modes of sound occur for given qin superfluid ^{4}He. Details will be provided in a forthcoming paper.

REFERENCES

1. Kampf A.P. and Schrieffer J.R., *Phys. Rev. B* **41**, 6399(1990).
2. Aebi P., Osterwalder J., Schwaller P., Schlapbach L., Shimoda M., Mochiku T. and Kadowaki K., *Phys. Rev. Lett.* **72**, 2757 (1994).
3. Aebi P. et al., this volume.
4. Millis A.J., Monien H. and Pines D., *Phys. Rev. B32*, 167 (1990).
5. Dagotto E., Moreo A., Ortolani F., Poilblanc D. and Riera J.,*Phys. Rev. B45*, 10741, (1992); Dagotto E., Ortolani F. and Scalapino D.J., *Phys. Rev. B 46*, 3183 (1992).
6. Scalapino D.J., *Physica C185–188*, 104 (1991).